Received: 23 January 2018 | Revised: 28 April 2018 | Accepted: 2 May 2018
DOI: 10.1002/ardp.201800017

FULL PAPER

DPhG ARCH PHARM
Archiv der Pharmazie

Expanding the chemical space of anti-HCV NS5A inhibitors by stereochemical exchange and peptidomimetic approaches

Triveena M. Ramsis[1] | Shereen E. Abdel Karim[1] | Niki Vassilaki[2] | Efseveia Frakolaki[2] | Ahmed A. M. Kamal[3] | Grigoris Zoidis[4] | Nermin S. Ahmed[1] | Ashraf H. Abadi[1]

[1] Faculty of Pharmacy and Biotechnology, Department of Pharmaceutical Chemistry, German University in Cairo, Cairo, Egypt

[2] Molecular Virology Laboratory, Hellenic Pasteur Institute, Athens, Greece

[3] Pharmaceutical and Medicinal Chemistry, Department of Drug Design Optimization, Saarland University and Helmholtz Institute for Pharmaceutical Research Saarland (HIPS), Saarbrücken, Germany

[4] Faculty of Pharmacy, Department of Pharmaceutical Chemistry, School of Health Sciences, National and Kapodistrian University of Athens, Athens, Greece

Correspondence
Prof. Ashraf H. Abadi, Faculty of Pharmacy and Biotechnology, Department of Pharmaceutical Chemistry, German University in Cairo, 11835 Cairo, Egypt.
Email: ashraf.abadi@guc.edu.eg

Funding information
Science and Technology Development Fund (Egypt), Grant number: 22848

Abstract

Here we report a series of potent anti-HCV agents bearing a symmetrical benzidine L-prolinamide backbone with different capping groups including alkyl/aryl carbamates of natural and unnatural valine and leucine amino acids. All compounds were investigated for their inhibitory activity in an HCV replicon assay on genotype 1b. The novel compounds share some chemical and clinical attributes of commercially available NS5A inhibitors. Compounds **5** and **6** with unnatural capping residue and ethyl and isobutyl carbamates showed EC_{50} values in the picomolar range with a low toxicity profile and selectivity indices of several orders of magnitude. These findings enlarge the chemical space from which NS5A inhibitors may be discovered by adopting unnatural amino acids, amino acids other than valine and carbamates other than methyl as the capping groups.

KEYWORDS
anti-HCV, bivalent ligands, NS5A inhibitors, peptidomimetics

1 | INTRODUCTION

Hepatitis C virus (HCV) is the leading cause of chronic liver disease worldwide as well as the primary cause of liver transplantations. The World Health Organization (WHO) estimates that about 3% of the world's population, i.e., 170 million people, is currently infected with HCV.[1] Each year, 3 to 4 million people are newly infected with HCV.[2] The pathogen causes significant morbidity, with approximately 399000 deaths per year as a direct result of complications involved in end-stage liver diseases.[3] Most of the infected individuals (~80%) will develop chronic infection, the latter is often associated with the development of hepatitis, steatosis, fibrosis, and liver cirrhosis. HCV is currently classified into six main genotypes (identified as 1 through 6), with 31–33% nucleotide sequence divergence. Each genotype is further divided into subtypes (designated by lower case letters), with each subtype differing from one another by 20–25%.[4] The combination of molecular cloning and development of a replicon assay has enabled the discovery of novel DAAs targeting viral proteins.[5,6] HCV is an enveloped positive-stranded RNA virus, the RNA is translated into a polyprotein consisting of 10 proteins. This polyprotein is then processed by both cellular and viral proteases to form three structural (S) elements (core [C], E1, and E2), and seven non-structural (NS) proteins (p7, NS2, NS3, NS4A, NS4B, NS5A, and NS5B). NS5A is a hydrophilic phosphoprotein containing an N-terminal amphipathic α-helix that mediates virus association with the ER membrane. This phosphoprotein exists in two forms: a basally

phosphorylated form and a hyperphosphorylated form.[7–10] NS5A is also a multi-functional protein with no apparent enzymatic activity.

NS5A is proposed to be involved in resistance to the host immune response, and is an essential component of the viral lifecycle with involvement in replication and maturation/packaging of the viral genome.[6] Until 2011, the combination of pegylated interferon-α (PEG-IFN-α) and ribavirin regimen for a duration of 24 or 48 weeks has been the standard of care for the treatment of HCV.[5] However, in 2014, daclatasvir (**I**) was the first NS5A inhibitor to be introduced to the market and used in HCV treatment (Figure 1). Ombitasvir (**II**) and ledipasvir were subsequently introduced to the market (Figure 1). Here we report a class of symmetric bivalent ligands bearing a benzidine L-prolinamide scaffold. The novel series is designed to keep the previously reported pharmacophoric features of NS5A inhibitors, namely the two aromatic hydrophobic regions, a hydrophobic terminal chain and at least two hydrogen bond acceptors.[11]

2 | RESULTS AND DISCUSSION

2.1 | Chemistry

Coupling of benzidine with Boc-L-proline using EEDQ resulted in a pure Boc-protected product which was deprotected using trifluouroacetic acid (TFA). A series of capping groups were coupled to the free amine using HBTU. The capping groups are carbamate derivatives prepared from a series of commercially available amino acid enantiomers, using different chloroformates in NaOH and in high yields (Schemes 1 and 2).

2.2 | Biology

Compounds **1–16** were tested for their EC_{50}, EC_{90}, and CC_{50} using luciferase reporter replicon assay on genotype 1b, CON-1 strain. In addition, selected compounds were also tested on genotype 2a, JFH-1 strain. The cell line used for virus replication was human hepatoma cell line (Huh-7). EC_{50} is the compound concentration reducing the virus replication in Huh-7 infected cells by 50%, CC_{50} is the compound concentration decreasing the cell viability of non-infected Huh-7 by 50%, SI_{50} is the ratio of CC_{50}/EC_{50} and it indicates the safety of the compound as antiviral agent. The results are summarized in Tables 1 and 2.

All 16 compounds in Table 1 had the benzidine L-prolinamide part unchanged while we adopted capping groups of *R*- and *S*-valine and leucine containing different alkyl/aryl carbamate esters (Figure 1).

Although the molecule is structurally symmetric, the non-coplanarity of the two phenyl rings of benzidine may lead to

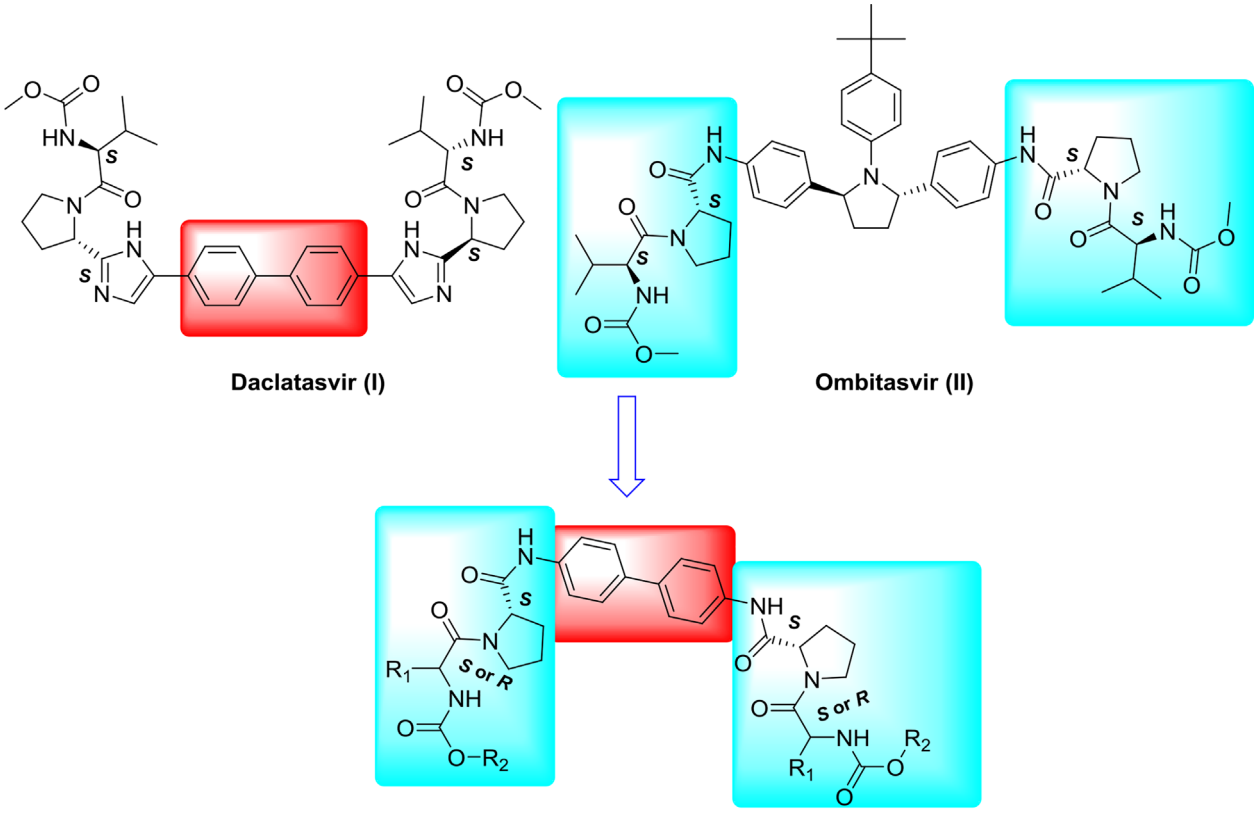

FIGURE 1 Structures of the clinically available daclatasvir (**I**), ombitasvir (**II**) and the scaffold of newly synthesized compounds **1–16**

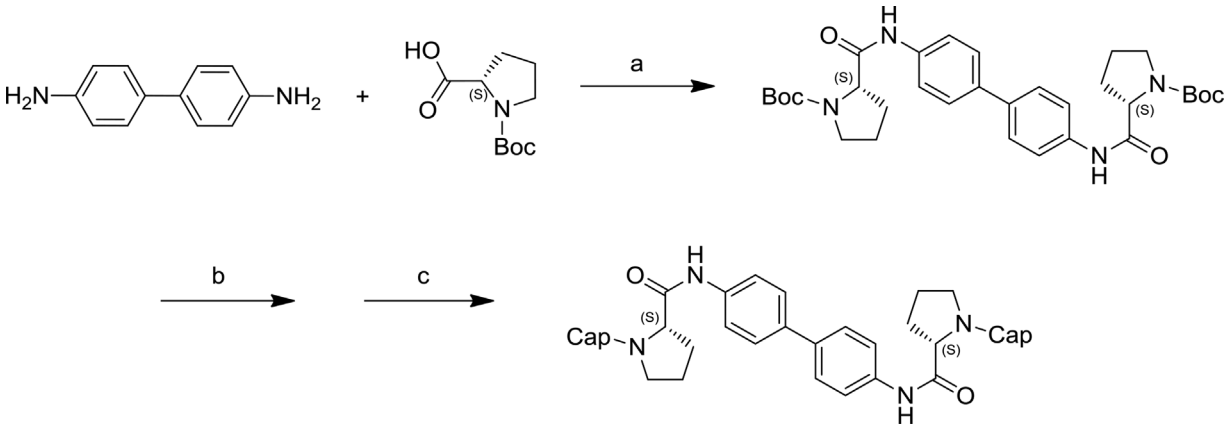

SCHEME 1 (a) *N*-Boc-L-proline, EEDQ, CH_2Cl_2; (b) TFA, CH_2Cl_2; (c) capping group, HBTU, DIPEA, CH_2Cl_2

asymmetric binding to the receptor and different projections of the side chains in space, Figure 2.

For most of the clinically used NS5A inhibitors, the capping group on the nitrogen of the proline/proline-like moiety is *S*-valine methyl carbamate ester. The assay data indicate that the inhibitory activity of these analogues is greatly dependent upon the structure of the terminal capping groups.

Surprisingly, in the case of molecules with valine amino acids **1–4** and **9–12**, the higher activity is limited to the *R*-epimers **1–4**. This is a new finding and indicates the value of testing both natural and unnatural epimers of the same residue to decide about the more active derivatives.

Among the ethyl, isobutyl, butyl, and benzyl carbamates of **1–4** and **9–12**, the most active derivatives are the benzyl carbamates **4** and **12**. This indicates that this moiety is mostly involved in hydrophobic interaction with the receptor.

Among the leucine derivatives **5–9** and **13–16**, again the *R*-epimers derivatives are more active than the *S*-epimers; this confirms the crucial role of the stereocenter of the AA residue and the important role of the projection plane upon activity.[12]

The higher activities of the *R*-epimers relative to the *S*-epimers for those molecules doubles the chemical space from which new NS5A inhibitors can be discovered. This also confirms the essential role of stereochemical centre on the capping group, with an obvious favor to *R* configuration.

As per the carbamate moiety of the *R*-epimer derivatives **9–12**, the higher activity has been more associated with the small alkyls ethyl **9**, or aromatic benzyl **12** rather than longer and bulkier isobutyl **10** and butyl **11** terminal chains (Table 1).

Within the *R*-epimer series **1–8**, the *R*-leucine containing compounds have been more active than the *R*-valine ones. These results indicate the success of our peptidiomimetic principle regarding the use of unnatural capping residue and the development of active analogues with capping groups bearing an *R*-configuration, both approaches widen the scope for development of new clinically effective DAAs.

Most of the synthesized molecules were not cytotoxic at the highest concentration tested; this leads to SI_{50}s of several orders of magnitude, for example compounds **5** and **6** showed SI_{50} values of 86523 and >71428 and SI_{90} values of 6200 and >6020, respectively.

Within the tested concentration ranges, the EC_{50}s of compounds **5** and **6** as well as their CC_{50} and SI_{50} values against genotype 2a displayed improved antiviral values in comparison to sofosbuvir which was included as positive control in our assay.

Compounds **1–3** have shown nanomolar EC_{50} values on genotype 2a; this may indicate a promising pan genotypic activity of the novel compounds.

To date all NS5A inhibitors were identified through cell-based replicon assays. An X-ray of the NS5A protein co-crystallized with daclatasvir (**I**), or any approved inhibitor, has never been established, that is why daclatasvir and its clinically related compounds are described as NS5A replication complex inhibitors. Thus, we have defined the binding pocket guided by previous literature,[11] reported resistance mutations, and automatic site finder of the software MOE 2015.[13]

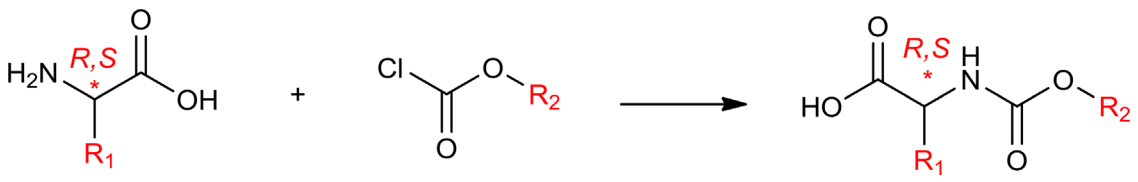

SCHEME 2 Synthesis of capping groups

TABLE 1 Replicon assay results for compounds **1–8** against HCV genotype 1b

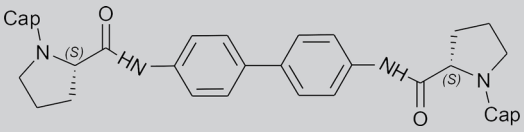

Cpd #	Capping groups	Stereochemistry	EC_{50} (nM)	EC_{90} (nM)	CC_{50} (nM)	SI_{50}	SI_{90}
1	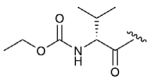	*R*	130	260	>20000	>154	>76
2	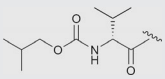	*R*	350	610	11250	32	18
3	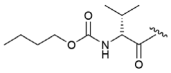	*R*	20	60	6320	316	105
4	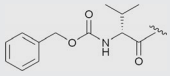	*R*	17.4	115	>20000	>1149	>174
5	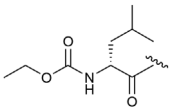	*R*	0.21	2.90	18170	86523	6200
6	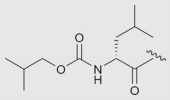	*R*	0.28	3.30	>20000	>71428	>6060
7	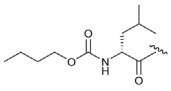	*R*	1.35	7.9	>20000	>14814	>2532
8	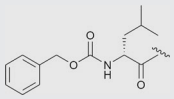	*R*	4.83	37.5	>20000	>4140	>533
9	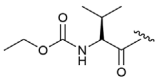	*S*	3700	13000	>20000	>5.4	>1.5
10	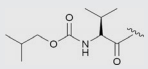	*S*	>20000	>20000	>20000	1	1
11	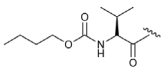	*S*	>20000	>20000	>200000	1	1
12	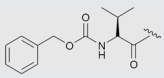	*S*	580	4000	>100000	>170	>25
13	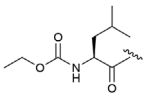	*S*	7200	>20000	>20000	>3	1
14	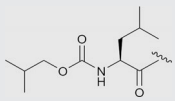	*S*	>20000	>20000	>20000	1	1
15	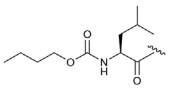	*S*	>20000	>20000	>20000	1	1

(Continues)

TABLE 1 (Continued)

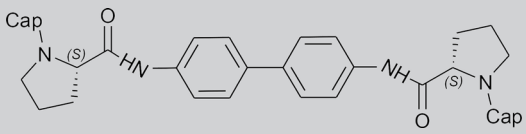

Cpd #	Capping groups	Stereochemistry	EC_{50} (nM)	EC_{90} (nM)	CC_{50} (nM)	SI_{50}	SI_{90}
16	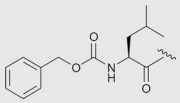	*S*	6100	>10000	>10000	>1.6	1
	Sofosbuvir		70	300	>5000	>71	>17

Docking of compounds **5** (EC_{50} = 0.21 nM), and daclatasvir (**I**), using the closed conformer of NS5A (PDB ID: 3FQM), showed that the two compounds bind to the binding pocket with nearly the same pose. The 2D interactions of the two molecules showed hydrogen bonding with Gln54 (Figure 3A–C).

3 | CONCLUSION

The chemical space of NS5A inhibitors can be extrapolated beyond the methylcarbamate of l-valine. The dynamic and kinetics of new derivatives with unnatural amino acids is still to be investigated. To further confirm that the novel compounds act via inhibiting NS5A protein, more replicon assays are required using resistant NS5A variant, this can validate NS5A as the potential target of the novel bivalent compounds.

4 | EXPERIMENTAL

4.1 | Chemistry

4.1.1 | General

All starting materials and solvents were obtained from commercial suppliers, and were used without further purification. Melting points were determined on a Büchi B-540 melting point apparatus and are uncorrected. ^{1}H NMR spectra were recorded at 300 MHz using Varian Mercury VX-300 MHz spectrometer. ^{13}C NMR spectra were recorded at 126 MHz using a Bruker DRX-126 MHz spectrometer. The solvents used were DMSO-d_6 or $CDCl_3$. Chemical shifts are given in parts per million (ppm), and all coupling constants (*J*) are given in Hz. The purities of the tested compounds were determined by HPLC coupled with mass spectrometry and were all higher than 95% purity unless otherwise indicated. Mass spectrometric analysis (HPLC-ESI-MS) was performed on a TSQ quantum (Thermo Electron Corporation) instrument equipped with an ESI source and a triple quadrupole mass detector. All masses were reported as $[M+H]^+$. Column chromatography was performed using silica gel 70–230 mesh. Reaction progress was monitored by TLC using fluorescent pre-coated silica gel plates and detection of the components was made by short UV light (λ = 254 nm). Reactions were carried out under argon when needed.

The InChI codes of the investigated compounds together with some biological activity data are provided as Supporting Information.

4.1.2 | General procedures for the preparation of the amino acid carbamates[14]

Distilled H_2O (100 mL) and NaOH (100 mmol, 4.0 g) were added to a 500 mL round bottom flask equipped with a magnetic stirring bar and the solution was cooled to 0°C in an ice bath. The appropriate amino acid (35 mmol) was added and stirred until a homogeneous solution

TABLE 2 Replicon assay results for compounds **1–3** against HCV genotype 2a

Cpd #	Capping groups	Stereochemistry	EC_{50} (nM)	EC_{90} (nM)	CC_{50} (nM)	SI_{50}	SI_{90}
1	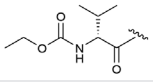	*R*	610	5340	>20000	>33	>4
2	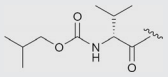	*R*	450	1730	>20000	>44	>12
3	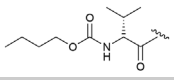	*R*	550	11250	>20000	87	20

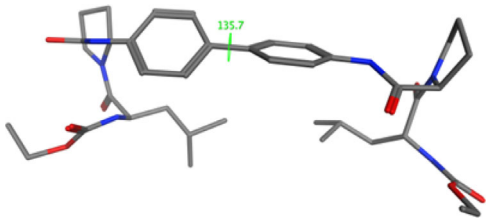

FIGURE 2 Showing non-coplanarity of the two core phenyls with dihyderal angle of 135.7°

was obtained. The corresponding chloroformate (45.5 mmol) in 1,4-dioxane (40 mL) was added dropwise through an addition funnel. The reaction mixture was then allowed to stir at room temperature overnight. The solution was extracted with Et_2O (3 × 50 mL), and the organic layers were discarded. The aqueous layer was again cooled to 0°C in an ice bath, and concentrated HCl was added dropwise until pH = 2. The aqueous solution was again extracted with Et_2O (3 × 50 mL). The aqueous layer was discarded and the organic layers were combined, dried over anhydrous Na_2SO_4, filtered, and concentrated *in vacuo* to give the crude product as clear viscous oil. Further purification was not required.

4.1.3 | General procedures for the *N*-protected benzidine prolinamide[12]

EEDQ (91.3 mmol) was added to a stirred solution of *N*-Boc-L-proline (18.83 g, 87.5 mmol) and benzidine (38.1 mmol) in dry CH_2Cl_2 (250 mL). The mixture was stirred at room temperature for 16 h under N_2. The volatile component was removed *in vacuo*. The residue was washed with Et_2O and suction-filtered to provide the respective compounds as white solid with >95% yield. Further purification was not required.

4.1.4 | General procedures for the deprotected benzidine prolinamide[15]

N-Boc-proline intermediates (0.04 mol) in CH_2Cl_2 were treated with CF_3CO_2H (60 mL) at room temperature under N_2. The mixture was stirred for 3 h before additional CF_3CO_2H (24 mL) was added. After being stirred for an additional 4 h period at room temperature, the volatile component was evaporated *in vacuo*. The residue was then dissolved in EtOAc, washed with saturated $NaHCO_3$ solution and brine. Some 1 N NaOH was added till pH reached 12. After that, the residue was dried over anhydrous Na_2SO_4. EtOAc was evaporated *in vacuo* to give a pale yellow sticky solid. This semi-solid was dissolved in acetone and evaporated *in vacuo*. This step was repeated two to three times to give a pale yellow crystalline solid. Further purification was not required.

4.1.5 | General procedures for the preparation of the final compounds (1–16)[12]

Deprotected benzidine prolinamide (0.003 mol) was added to the amino acid carbamates (0.4 g, 0.001 mol), HBTU (1.13 g, 0.003 mol) and DIPEA (0.7 mL) in CH_2Cl_2. The reaction mixture was stirred for 2 h at room temperature under N_2. The volatile component was removed *in vacuo*. The residue was then purified using silica gel column chromatography (98.5:1.5 CH_2Cl_2/MeOH) to provide compounds **1**–**16**.

Diethyl((2*R*,2′*R*)-((2*S*,2′*S*)-2,2′-(([1,1′-biphenyl]4,4′diylbis(azane-diyl))bis(carbonyl))bis(pyrrolidine-2,1diyl))bis(3-methyl-1-oxobut-ane-2,1-diyl))dicarbamate (1)

Dark brown semi-solid; yield: 26.4%; $C_{38}H_{52}N_6O_8$; FT-IR (cm^{-1}): 3210 (N-H), 1692 (C═O), 1640 (C═O), 1602 (CO); LC/MS: $[M+H]^+$ = 721; purity 95%; ^1H NMR (300 MHz, $CDCl_3$) δ 9.25 (s, 2H), 7.58 (d, *J* = 8.2 Hz, 4H), 7.38 (d, *J* = 8.4 Hz, 4H), 5.35 (d, *J* = 8.2 Hz, 2H), 4.76 (d, *J* = 6.4 Hz, 2H), 4.26 (t, *J* = 7.9 Hz, 2H), 4.17–3.95 (m, 6H), 3.70–3.56 (m, 2H), 2.49 (s, 2H), 2.17 (s, 2H), 2.10–1.97 (m, 6H), 1.20 (t, *J* = 7.1 Hz, 6H), 1.03 (dd, *J* = 6.7, 3.3 Hz, 12H); ^{13}C NMR (126 MHz, $CDCl_3$): δ 179.13, 174.58, 156.57, 136.00, 126.53, 126.38, 120.34, 61.36, 58.81, 46.95, 31.10, 19.11, 17.44, 14.58, 8.80.

Diisobutyl((2*R*,2′*R*)-((2*S*,2′*S*)-2,2′-(([1,1′-biphenyl]-4,4′ diylbis(azanediyl))bis(carbonyl))bis(pyrrolidine-2,1-diyl))bis(3-methyl-1-oxobutane-2,1-diyl))dicarbamate (2)

Dark brown semi-solid; yield: 25%; $C_{42}H_{60}N_6O_8$; FT-IR (cm^{-1}): 3210 (N-H), 1676 (C═O), 1635 (C═O), 1610 (C═O); LC/MS: $[M+H]^+$ = 777; purity 95%; ^1H NMR (300 MHz, $CDCl_3$): δ 9.07 (s, 2H), 7.65 (d, *J* = 8.4 Hz, 4H), 7.45 (d, *J* = 8.2 Hz, 4H), 5.28 (s, 2H), 4.77 (d, *J* = 6.9 Hz, 2H), 4.47 (s, 2H), 4.01 (s, 2H), 3.81 (d, *J* = 6.5 Hz, 4H), 3.53 (d, *J* = 8.0 Hz, 2H), 2.09 (s, 8H), 1.90–1.71 (m, 2H), 1.63 (dd, *J* = 11.5, 7.1 Hz, 2H), 1.00 (dd, *J* = 6.5, 2.6 Hz, 12H), 0.86 (t, *J* = 7.4 Hz, 12H); ^{13}C NMR (126 MHz, $CDCl_3$): δ 173.22, 169.00, 157.30, 137.31, 136.49, 126.99, 120.53, 61.32, 51.52, 47.26, 40.85, 27.98, 25.56, 24.25, 22.41, 21.87, 19.26, 19.01.

Dibutyl((2*R*,2′*R*)-((2*S*,2′*S*)-2,2′-(([1,1′-biphenyl]-4,4′ diylbis(azanediyl))bis(carbonyl))bis(pyrrolidine-2,1-diyl))bis(3-methyl-1-oxo-butane-2,1-diyl))dicarbamate (3)

Off-white solid; yield: 25%; mp: 81–82°C; $C_{42}H_{60}N_6O_8$; FT-IR (cm^{-1}): 3211 (N-H), 1689 (C═O), 1631 (C═O), 1600 (C═O); LC/MS: $[M+H]^+$ = 777; purity 95%; ^1H NMR (300 MHz, $CDCl_3$): δ 9.07 (s, 2H), 7.66 (d, *J* = 8.3 Hz, 4H), 7.44 (d, *J* = 8.3 Hz, 4H), 5.39 (s, 2H), 4.76 (d, *J* = 6.8 Hz, 2H), 4.46 (s, 2H), 4.02 (dd, *J* = 14.5, 7.0 Hz, 6H), 3.14 (s, 6H), 2.51 (s, 2H), 2.07 (s, 4H), 1.52 (td, *J* = 13.7, 6.7 Hz, 8H), 0.99 (dd, *J* = 6.3, 2.8 Hz, 12H), 0.86 (t, *J* = 7.3 Hz, 6H); ^{13}C NMR (126 MHz, $CDCl_3$) δ 172.96, 169.01, 157.59, 136.96, 127.56, 126.98, 120.65, 65.55, 61.28, 58.68, 47.02, 28.60, 24.57, 19.03, 8.79.

Dibenzyl((2*R*,2′*R*)-((2*S*,2′*S*)-2,2′-(([1,1′-biphenyl]-4,4′-diylbis(azanediyl))bis(carbonyl))bis(pyrrolidine-2,1-diyl))bis(3-methyl-1-oxo-butane-2,1-diyl))dicarbamate (4)

Pale yellow solid; yield: 34.5%; mp: 109–111°C; $C_{48}H_{56}N_6O_8$; FT-IR (cm^{-1}): 3300 (N-H), 1694 (C═O), 1631 (CO), 1605 (C═O); LC/MS: $[M+H]^+$ = 845; purity 95%; ^1H NMR (300 MHz, $CDCl_3$): δ 9.19 (s, 2H), 7.60 (d, *J* = 8.6 Hz, 4H), 7.41 (d, *J* = 8.6 Hz, 4H), 7.28

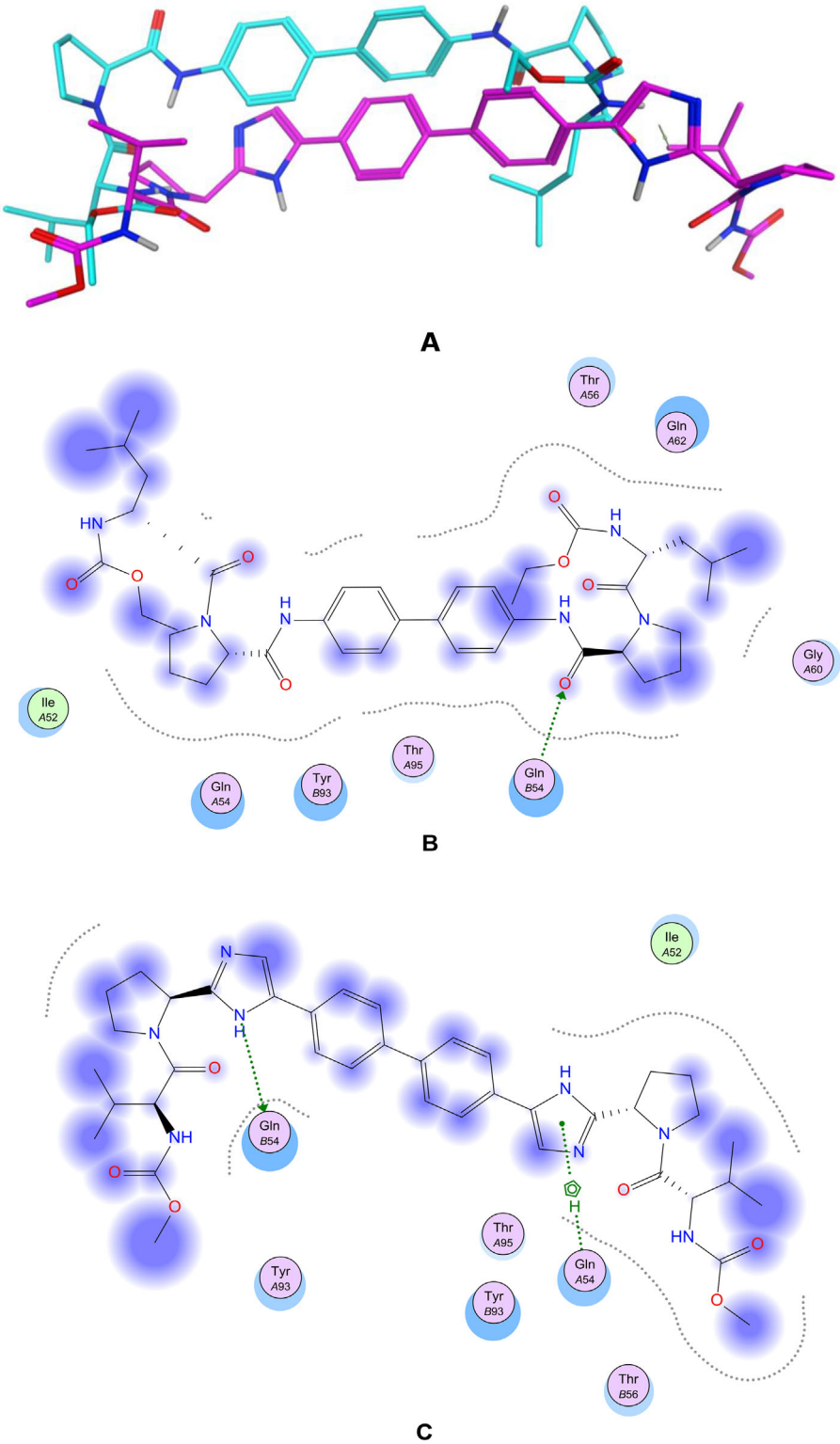

FIGURE 3 (A) An overlay of the best docked poses of compound **5** (cyan) and daclatasvir (pink), in the receptor binding pocket. The receptor and polar hydrogens were removed for clarity. (B and C) The 2D ligand interaction shows interaction by hydrogen bonding between the amide or imidazole with residue Gln54

(d, J = 3.0 Hz, 10H), 5.41 (s, 2H), 5.06 (dd, J = 32.7, 12.3 Hz, 4H), 4.78 (d, J = 7.7 Hz, 2H), 4.26 (s, 2H), 3.60 (s, 4H), 2.55 (s, 2H), 2.12–1.99 (m, 8H), 1.05–1.01 (m, 12H); ^{13}C NMR (126 MHz, $CDCl_3$) δ 172.52, 168.93, 156.82, 137.28, 136.32, 128.29, 127.61, 126.83, 120.29, 67.41, 61.19, 58.42, 47.70, 30.89, 24.67, 19.50, 18.26.

Diethyl((2*R*,2′*R*)-((2*S*,2′*S*)-2,2′-(([1,1′-biphenyl]-4,4′-diylbis(azanediyl))bis(carbonyl))bis(pyrrolidine-2,1-diyl))bis(4-methyl-1-oxo-pentane-2,1-diyl))dicarbamate (5)

Pale yellow solid; yield: 28%; mp: 127–129°C; $C_{40}H_{56}N_6O_8$; FT-IR (cm^{-1}): 3275 (N-H), 1689 (CO), 1632 (C═O), 1600 (C═O); LC/MS: $[M+H]^+$ = 748; purity 99%; ^{1}H NMR (300 MHz, $CDCl_3$): δ 9.09 (s, 2H), 7.65 (d, *J* = 8.2 Hz, 4H), 7.45 (d, *J* = 8.4 Hz, 4H), 5.32 (s, 2H), 4.77 (d, *J* = 6.5 Hz, 2H), 4.48 (s, 2H), 4.17–3.94 (m, 6H), 3.53 (d, *J* = 7.8 Hz, 2H), 1.99 (s, 8H), 1.76 (s, 2H), 1.63 (t, *J* = 11.7 Hz, 2H), 1.47 (s, 2H), 1.20 (t, *J* = 7.1 Hz, 6H), 1.00 (dd, *J* = 6.4, 4.2 Hz, 12H); ^{13}C NMR (126 MHz, $CDCl_3$): δ 173.21, 169.00, 157.11, 137.34, 136.39, 126.98, 120.44, 61.35, 51.48, 47.44, 40.98, 28.39, 24.66, 21.84, 14.57.

Diisobutyl((2*R*,2′*R*)-((2*S*,2′*S*)-2,2′-(([1,1′-biphenyl]-4,4′-diylbis(azanediyl))bis(carbonyl))bis(pyrrolidine-2,1-diyl))bis(4-methyl-1-oxo-pentane-2,1-diyl))dicarbamate (6)

Pale yellow solid; yield: 25%; mp: 117–118°C; $C_{44}H_{64}N_6O_8$; FT-IR (cm^{-1}): 3282 (N-H), 1689 (C═O), 1633 (C═O), 1603 (C═O); LC/MS: $[M+H]^+$ = 804; purity 100%; ^{1}H NMR (300 MHz, $CDCl_3$): δ 9.07 (s, 2H), 7.65 (d, *J* = 8.4 Hz, 4H), 7.45 (d, *J* = 8.2 Hz, 4H), 5.28 (s, 2H), 4.77 (d, *J* = 6.9 Hz, 2H), 4.47 (s, 2H), 4.01 (s, 2H), 3.81 (d, *J* = 6.5 Hz, 4H), 3.53 (d, *J* = 8.0 Hz, 2H), 2.09 (s, 8H), 1.90–1.71 (m, 6H), 1.63 (dd, *J* = 11.5, 7.1 Hz, 2H), 1.00 (dd, *J* = 6.5, 2.6 Hz, 12H), 0.86 (t, *J* = 7.4 Hz, 12H); ^{13}C NMR (126 MHz, $CDCl_3$): δ 173.22, 169.00, 157.30, 137.31, 136.49, 127.17, 120.53, 61.32, 51.52, 47.26, 40.85, 27.98, 24.25, 23.37, 22.41, 19.01.

Dibutyl((2*R*,2′*R*)-((2*S*,2′*S*)-2,2′-(([1,1′-biphenyl]-4,4′-diylbis(azanediyl))bis(carbonyl))bis(pyrrolidine-2,1-diyl))bis(4-methyl-1-oxo-pentane-2,1-diyl))dicarbamate (7)

Pale yellow solid; yield: 24%; mp: 85–87°C; $C_{44}H_{64}N_6O_8$; FT-IR (cm^{-1}): 3300 (N-H), 1688 (CO), 1631 (CO), 1601 (C═O); LC/MS: $[M+H]^+$ = 804; purity 99%; ^{1}H NMR (300 MHz, $CDCl_3$): δ 9.07 (s, 2H), 7.66 (d, *J* = 8.3 Hz, 4H), 7.44 (d, *J* = 8.3 Hz, 4H), 5.39 (s, 2H), 4.76 (d, *J* = 6.8 Hz, 2H), 4.46 (s, 2H), 4.02 (dd, *J* = 14.5, 7.0 Hz, 6H), 3.14 (s, 6H), 2.51 (s, 2H), 2.07 (s, 6H), 1.76 (s, 2H), 1.52 (td, *J* = 13.7, 6.7 Hz, 8H), 0.99 (dd, *J* = 6.3, 2.8 Hz, 12H), 0.86 (t, *J* = 7.3 Hz, 6H); ^{13}C NMR (126 MHz, $CDCl_3$): δ 173.28, 169.08, 157.30, 137.29, 136.47, 126.97, 120.53, 65.52, 61.35, 51.51, 46.90, 40.78, 30.97, 28.25, 24.69, 23.46, 21.83, 19.04, 13.72, 9.00.

Dibenzyl((2*R*,2′*R*)-((2*S*,2′*S*)-2,2′-(([1,1′-biphenyl]-4,4′-diylbis(azanediyl))bis(carbonyl))bis(pyrrolidine-2,1-diyl))bis(4-methyl-1-oxo-pentane-2,1-diyl))dicarbamate (8)

Pale yellow solid; yield: 25%; mp: 81–83°C; $C_{50}H_{60}N_6O_8$; FT-IR (cm^{-1}): 3300 (N-H), 1693 (C═O), 1631 (CO), 1600 (C═O); LC/MS: $[M+H]^+$ = 872; purity: 95%; ^{1}H NMR (300 MHz, $CDCl_3$): δ 9.06 (s, 2H), 7.63 (d, *J* = 8.6 Hz, 4H), 7.43 (d, *J* = 8.6 Hz, 4H), 7.28 (d, *J* = 4.7 Hz, 10H), 5.42 (s, 2H), 5.07 (q, *J* = 12.2 Hz, 4H), 4.75 (d, *J* = 6.9 Hz, 2H), 4.50 (s, 2H), 4.00 (s, 2H), 3.53 (s, 2H), 2.99 (s, 2H), 2.55 (s, 4H), 2.09 (s, 6H), 1.76 (s, 2H), 1.00 (t, *J* = 5.4 Hz, 12H); ^{13}C NMR (126 MHz, $CDCl_3$): δ 173.19, 169.13, 156.30, 137.25, 128.29, 127.06, 120.52, 67.27, 61.28, 51.63, 46.94, 40.97, 28.26, 24.65, 8.79.

Diethyl((2*S*,2′*S*)-((2*S*,2′*S*)-2,2′-(([1,1′-biphenyl]-4,4′-diylbis(azanediyl))bis(carbonyl))bis(pyrrolidine-2,1-diyl))bis(3-methyl-1-oxo-butane-2,1-diyl))dicarbamate (9)

Yellow oil; yield: 20%; $C_{38}H_{52}N_6O_8$; FT-IR (cm^{-1}): 3248 (N-H), 1680 (CO), 1635 (C═O), 1619 (CO); LC/MS: $[M+H]^+$ = 777; purity 98%; ^{1}H NMR (300 MHz, $CDCl_3$) δ 9.50 (s, 2H), 7.40 (d, *J* = 8.2 Hz, 4H), 7.30 (d, *J* = 8.2 Hz, 4H), 5.28 (s, 2H), 4.78 (d, *J* = 5.3 Hz, 2H), 4.36 (d, *J* = 6.6 Hz, 2H), 4.16–4.04 (m, 4H), 3.80 (d, *J* = 8.6 Hz, 2H), 3.66 (s, 2H), 2.45 (s, 2H), 2.18 (s, 2H), 2.09–1.99 (m, 4H), 1.95 (s, 2H), 1.24 (t, *J* = 7.0 Hz, 12H), 1.00 (d, *J* = 6.7 Hz, 6H). ^{13}C NMR (126 MHz, $CDCl_3$) δ 175.22, 173.58, 155.55, 136.33, 126.53, 126.56, 121.05, 62.36, 59.07, 47.13, 31.10, 19.45, 18.14, 15.52, 9.00.

Diisobutyl((2*S*,2′*S*)-((2*S*,2′*S*)-2,2′-(([1,1′-biphenyl]-4,4′-diylbis(azanediyl))bis(carbonyl))bis(pyrrolidine-2,1-diyl))bis(3-methyl-1-oxo-butane-2,1-diyl))dicarbamate (10)

Dark yellow semi-solid; yield: 22%; $C_{42}H_{60}N_6O_8$; FT-IR (cm^{-1}): 3225 (N-H), 1680 (CO), 1632 (CO), 1622 (CO); LC/MS: $[M+H]^+$ = 777; purity 98%; ^{1}H NMR (300 MHz, DMSO) δ 10.08 (s, 2H), 7.62 (d, *J* = 8.6 Hz, 4H), 7.56 (d, *J* = 8.6 Hz, 4H), 4.41 (d, *J* = 23.8 Hz, 2H), 4.02 (t, *J* = 8.3 Hz, 2H), 3.86–3.76 (m, 4H), 3.71 (d, *J* = 6.7 Hz, 4H), 3.62 (s, 2H), 2.05–1.94 (m, 4H), 1.91–1.85 (m, 4H), 1.84–1.76 (m, 4H), 0.88–0.84 (m, 24H). ^{13}C NMR (126 MHz, DMSO) δ 170.73, 157.01, 138.68, 134.72, 126.88, 119.83, 70.42, 60.69, 59.95, 58.20, 46.37, 30.28, 29.95, 29.88, 28.11, 25.12, 19.59, 19.31, 19.04, 18.50.

Dibutyl((2*S*,2′*S*)-((2*S*,2′*S*)-2,2′-(([1,1′-biphenyl]-4,4′-diylbis(azanediyl))bis(carbonyl))bis(pyrrolidine-2,1-diyl))bis(3-methyl-1-oxo-butane-1,2-diyl))dicarbamate (11)

White solid; yield: 24%; mp: 100–103; $C_{42}H_{60}N_6O_8$; FT-IR (cm^{-1}): 3250 (N-H), 1689 (C═O), 1630 (CO), 1609 (C═O); LC/MS: $[M+H]^+$ = 777; purity 96%; ^{1}H NMR (300 MHz, DMSO) δ 10.02 (d, *J* = 22.5 Hz, 2H), 8.80 (s, 2H), 7.62 (d, *J* = 8.8 Hz, 4H), 7.56 (d, *J* = 8.8 Hz, 4H), 4.43 (dt, *J* = 15.4, 7.8 Hz, 2H), 4.08–3.98 (m, 2H), 3.97–3.85 (m, 4H), 3.78 (t, *J* = 11.6 Hz, 2H), 3.67–3.56 (m, 2H), 2.67 (s, 2H), 2.14 (dd, *J* = 12.6, 8.1 Hz, 2H), 1.99 (dd, *J* = 14.3, 8.2 Hz, 2H), 1.88 (dd, *J* = 15.4, 10.0 Hz, 4H), 1.57–1.40 (m, 4H), 1.38–1.24 (m, 4H), 0.93 (d, *J* = 6.7 Hz, 6H), 0.85 (dd, *J* = 15.1, 7.9 Hz, 12H). ^{13}C NMR (126 MHz, DMSO) δ 170.84, 156.91, 138.68, 134.75, 126.82, 119.77, 64.06, 60.64, 58.30, 47.65, 46.21, 38.68, 31.18, 30.26, 29.88, 25.13, 19.36, 19.00, 14.06, 9.08.

Dibenzyl((2*S*,2′*S*)-((2*S*,2′*S*)-2,2′-(([1,1′-biphenyl]-4,4′-diylbis(azanediyl))bis(carbonyl))bis(pyrrolidine-2,1-diyl))bis(3-methyl-1-oxo-butane-2,1-diyl))dicarbamate (12)

Yellow oil; yield: 25%; $C_{48}H_{56}N_6O_8$; FT-IR (cm^{-1}): 3285 (N-H), 1697 (C═O), 1625 (C═O), 1600 (CO); LC/MS: $[M+H]^+$ = 845; purity 95%; ^{1}H NMR (300 MHz, DMSO) δ 10.05 (d, *J* = 28.6 Hz, 2H), 7.62 (d, *J* = 8.7 Hz, 4H), 7.56 (d, *J* = 8.7 Hz, 4H), 7.39–7.22 (m, 10H), 5.19–4.85 (m, 4H), 4.45 (dd, *J* = 8.6, 5.3 Hz, 2H), 4.06 (t, *J* = 8.3 Hz, 2H), 3.80 (d, *J* = 6.2 Hz, 2H), 3.62 (d, *J* = 8.6 Hz, 2H), 2.10 (d, *J* = 32.2 Hz, 2H), 2.04–1.79 (m, 8H), 1.21 (s, 2H), 0.89 (dt, *J* = 30.8, 10.9 Hz, 12H). ^{13}C NMR (126 MHz, DMSO) δ 170.71, 156.54, 138.85, 137.47, 134.87, 128.78,

128.46, 128.21, 128.08, 126.83, 126.81, 119.94, 65.83, 60.64, 58.41, 30.29, 29.89, 25.12, 19.36, 19.02.

Diethyl((2*S*,2′*S*)-((2*S*,2′*S*)-(([1,1′-biphenyl]-4,4′-diylbis(azanediyl))bis(carbonyl))bis(pyrrolidine-2,1-diyl))bis(4-methyl-1-oxo-pentane-1,2-diyl))dicarbamate (13)

Yellow oil; yield: 30%; $C_{40}H_{56}N_6O_8$; FT-IR (cm^{-1}): 3275 (N-H), 1686 (C═O), 1633 (C═O), 1601 (CO); LC/MS: $[M+H]^+$ = 748; purity 95%; ^1H NMR (300 MHz, DMSO) δ 10.01 (s, 2H), 8.18 (s, 2H), 7.62 (d, *J* = 8.8 Hz, 4H), 7.58–7.54 (m, 4H), 4.50–4.39 (m, 2H), 4.27 (s, 2H), 3.95 (dt, *J* = 6.7, 3.4 Hz, 4H), 3.62–3.57 (m, 4H), 2.18–2.09 (m, 2H), 2.02 (dd, *J* = 12.2, 6.7 Hz, 2H), 1.96–1.83 (m, 4H), 1.66 (s, 2H), 1.48–1.38 (m, 4H), 1.15–1.11 (m, 6H), 0.91–0.86 (m, 12H). ^{13}C NMR (126 MHz, DMSO) δ 174.92, 170.85, 156.74, 138.70, 134.75, 126.80, 119.77, 60.20, 54.02, 52.41, 51.15, 47.12, 42.27, 24.73, 23.33, 21.56, 18.50, 17.17, 15.04, 12.91.

Diisobutyl((2*S*,2′*S*)-((2*S*,2′*S*)-(([1,1′-biphenyl]-4,4′-diylbis(azanediyl))bis(carbonyl))bis(pyrrolidine-2,1-diyl))bis(4-methyl-1-oxo-pentane-1,2-diyl))dicarbamate (14)

Brownish oil; yield: 24.4%; $C_{44}H_{64}N_6O_8$; FT-IR (cm^{-1}): 3282 (N-H), 1686 (CO), 1630 (CO), 1605 (C═O); LC/MS: $[M+H]^+$ = 804; purity 100%; ^1H NMR (300 MHz, $CDCl_3$) δ 10.07 (s, 2H), 7.65 (d, *J* = 8.4 Hz, 4H), 7.35 (d, *J* = 8.3 Hz, 4H), 5.40 (s, 2H), 4.64 (d, *J* = 6.6 Hz, 2H), 4.40 (s, 2H), 4.01 (s, 2H), 3.77 (d, *J* = 6.4 Hz, 4H), 3.47 (d, *J* = 8.0 Hz, 2H), 2.11 (s, 8H), 1.92–1.77 (m, 6H), 1.66 (dd, *J* = 11.0, 7.1 Hz, 2H), 1.00 (dd, *J* = 6.3, 2.6 Hz, 12H), 0.88 (t, *J* = 7.6 Hz, 12H). ^{13}C NMR (126 MHz, DMSO) δ 170.34, 156.33, 138.14, 134.26, 126.31, 125.05, 119.31, 76.39, 69.78, 60.13, 50.66, 45.72, 29.23, 27.60, 24.65, 24.06, 23.13, 21.27, 18.80, 8.58.

Dibutyl((2*S*,2′*S*)-((2*S*,2′*S*)-2,2′-(([1,1′-biphenyl]-4,4′-diylbis(azanediyl))bis(carbonyl))bis(pyrrolidine-2,1-diyl))bis(4-methyl-1-oxo-pentane-2,1-diyl))dicarbamate (15)

Pale white solid; yield: 26%; mp: 105–107°C; $C_{44}H_{64}N_6O_8$; FT-IR (cm^{-1}): 3280 (N-H), 1685 (C═O), 1636 (C═O), 1610 (CO); LC/MS: $[M+H]^+$ = 804; purity 98%; ^1H NMR (300 MHz, $CDCl_3$) δ 9.16 (s, 2H), 7.76 (d, *J* = 8.2 Hz, 4H), 7.54 (d, *J* = 8.5 Hz, 4H), 5.36 (s, 2H), 4.56 (d, *J* = 6.6 Hz, 2H), 4.30 (s, 2H), 4.02 (dd, *J* = 14.4, 7.2 Hz, 6H), 3.22 (s, 6H), 2.60 (s, 2H), 2.10 (s, 6H), 1.78 (s, 2H), 1.45 (td, *J* = 13.5, 6.4 Hz, 8H), 1.01 (dd, *J* = 6.2, 2.6 Hz, 12H), 0.86 (t, *J* = 7.2 Hz, 6H). ^{13}C NMR (126 MHz, $CDCl_3$) δ 174.42, 168.68, 157.25, 138.09, 136.57, 127.07, 121.33, 65.74, 61.58, 52.48, 46.98, 41.64, 31.20, 27.09, 24.80, 23.23, 22.00, 18.88, 13.58, 8.90.

Dibenzyl((2*S*,2′*S*)-((2*S*,2′*S*)-(([1,1′-biphenyl]-4,4′-diylbis(azanediyl))bis(carbonyl))bis(pyrrolidine-2,1-diyl))bis(4-methyl-1-oxo-pentane-1,2-diyl))dicarbamate (16)

Yellow oil; yield: 29%; $C_{38}H_{52}N_6O_8$; FT-IR (cm^{-1}): 3294 (N-H), 1689 (CO), 1636 (C═O), 1608 (CO); LC/MS: $[M+H]^+$ = 872; purity 95%; ^1H NMR (300 MHz, DMSO) δ 10.11 (s, *J* = 61.3 Hz, 2H), 7.62 (d, *J* = 8.7 Hz, 4H), 7.56 (d, *J* = 8.7 Hz, 4H), 7.35–7.28 (m, 10H), 4.96 (d, *J* = 29.6 Hz, 4H), 4.45 (dd, *J* = 8.2, 4.9 Hz, 2H), 4.34–4.17 (m, 2H), 3.68 (dd, *J* = 19.4, 12.3 Hz, 2H), 3.60–3.48 (m, 2H), 2.22–2.07 (m, 2H), 2.07–1.95 (m, 2H), 1.89 (ddd, *J* = 17.2, 11.9, 5.9 Hz, 4H), 1.65 (d, *J* = 9.7 Hz, 4H), 1.53–1.33 (m, 4H), 0.88 (d, *J* = 6.6 Hz, 12H). ^{13}C NMR (126 MHz, DMSO) δ 171.14, 170.83, 156.60, 138.65, 137.57, 134.61, 128.77, 128.46, 128.22, 128.12, 126.78, 119.80, 65.64, 63.23, 60.47, 51.25, 47.39, 29.66, 25.23, 24.47, 23.55, 21.71.

4.2 | Biology

4.2.1 | HCV anti-viral activity using genotype 1b, CON-1 strain replicon and genotype 2a, JFH-1 strain replicon[16–18]

Huh-7 cells were cultured in Dulbecco's modified Eagle's medium (DMEM) supplemented with 10% heat-inactivated fetal bovine serum (FBS), 0.1 mM nonessential amino acids, and 1× penicillin-streptomycin-glutamine.

The cells were infected with replicons of HCV genotype 1b, BM4-5 FEO or genotype 2a, JFH-1 (GenBank accession number AB047639), containing a firefly luciferase-neomycompounds cin phosphotransferase fusion (FEO) protein. This has been accomplished by electroporation as previously described.[16] Compound activity assays were carried out using 10000 replicon cells per well on 96-well plates.[16] Compounds were added 24–120 h after transfection or infection with supernatant. Cells and compounds were then incubated for 72 or 120 h with all conditions run in triplicate. Each experiment was performed on three separate occasions.

4.2.2 | Determination of compounds cytotoxicity[19]

The cytotoxicity of compounds **1–16** on uninfected Huh-7 cells was determined using MTT method as described.[19] The 50% cytotoxicity concentration (CC_{50}) was calculated from the optical density data using nonlinear regression curve fitting to the 4-parameter logistic equation and GraphPad Prism 4 software.

4.3 | Molecular modeling

Docking experiments were implemented to dock compound **5** and daclatasvir (**I**) into the proposed active site of NS5A with the program MOE version 2015.10.12 Compounds were constructed into the MOE window, then a conformational search was done for each of them using systematic method, and the databases were saved. The Protein Data Bank (PDB) crystal structure of NS5A co-crystallized with any NS5A inhibitor was not available therefore the binding pocket was defined.[11] The PDB crystal structure of NS5A (PDB ID: 3FQM) was imported into MOE. The protein structure was protonated and atomic charges were assigned. The binding pocket was defined using the site finder feature, other residues involved in viral mutation were also included in the defined pocket namely Gln54, Tyr93, Thr95, and Pro97, additionally residues previously claimed to be involved in H-bonding/hydrophobic interaction with daclatasvir (**I**) were included. The binding pocket was selected and extended 4.5 Å around the pocket. A database of

compound **5** and daclatasvir (**I**) was prepared as .mdb file then docking into the defined pocket was launched. The poses of the ligand conformation were generated using Triangle Matcher; the scoring function used was London dG, with refinement using Force field.

ACKNOWLEDGMENTS

This project is partially financed by the Science and Technology Development Fund (STDF), Egypt, Grant No: 22848, to Ashraf H. Abadi. The authors are grateful to the authority of the National Institute of Allergic and Infectious Diseases (NIAID), Division of Microbiology and Infectious Diseases (DMID), Rockville, MD 20852, USA, and the Southern Research Institute (SRI), Alabama for performing the biological testing in part.

ORCID

Ashraf H. Abadi http://orcid.org/0000-0002-7433-261X

REFERENCES

[1] S. L. Chen, T. R. Morgan, *Int. J. Med. Sci.* **2006**, *3*, 47.
[2] V. Soriano, M. G. Peters, S. Zeuzem, *Clin. Infect. Dis.* **2009**, *48*, 313.
[3] WHO, Hepatitis C. http://www.who.int/mediacentre/factsheets/fs164/en/ (accessed January 18, **2018**).
[4] P. Simmonds, J. Bukh, C. Combet, G. Deléage, N. Enomoto, S. Feinstone, P. Halfon, G. Inchauspé, C. kuiken, G. Maertens, M. Mizokami, D. G. Murphy, H. Okamoto, J. M. Paelotsky, F. penin, E. Sablon, T. Shin-I, L. j. Stuyver, H. J. Thiel, S. Viazov, A. J. Weiner, A. Widell, *Hepatology* **2005**, *42*, 962.
[5] J.-M. Pawlotsky, *Adv. Pharmacol.* **2013**, *67*, 169.
[6] V. Lohmann, F. Körner, J. Koch, U. Herian, L. Theilmann, R. Bartenschlager, *Science* **1999**, *285*, 110.
[7] T. Kaneko, Y. Tanji, S. Satoh, M. Hijikata, S. Asabe, K. Kimura, K. Shimotohno, *Biochem. Biophys. Res. Commun.* **1994**, *205*, 320.
[8] N. Appel, T. Pietschmann, R. Bartenschlager, *J. Virol.* **2005**, *79*, 3187.
[9] M. J. Evans, C. M. Rice, S. P. Goff, *Proc. Natl. Acad. Sci.* **2004**, *101*, 13038.
[10] P. Neddermann, M. Quintavalle, C. Di Pietro, A. Clementi, M. Cerretani, S. Altamura, L. Bartholomew, R. De Francesco, *J. Virol.* **2004**, *78*, 13306.
[11] K. H. Barakat, A. Anwar-Mohamed, J. A. Tuszynski, M. J. Robins, D. L. Tyrrell, M. Houghton, *J. Chem. Inf. Model.* **2015**, *55*, 362.
[12] I. H. Bae, J. K. Choi, C. Chough, S. J. Keum, H. Kim, S. K. Jang, B. M. Kim, *ACS Med. Chem. Lett.* **2014**, *5*, 255.
[13] M. O. E., Chemical Computing Group Inc., 1010 Sherbooke St. West, Suite #910, Montreal, QC, Canada, H3A 2R7, 2017.
[14] K. M. Engle, D.-H. Wang, J.-Q. Yu, *J. Am. Chem. Soc.* **2010**, *132*, 14137.
[15] D. R. St Laurent, M. H. Serrano-Wu, M. Belema, M. Ding, H. Fang, M. Gao, J. T. Goodrich, R. G. Krause, J. A. Lemm, M. Liu, O. D. Lopez, V. N. Nguyen, P. T. Nower, D. R 2nd O'Boyle, B. C. Pearce, J. L. Romine, L. Valera, J. H. Sun, Y. K. Wang, F. Yang, X. Yang, N. A. Meanwell, L. B. Snyder, *J. Med. Chem.* **2014**, *57*, 1976.
[16] D. L. Wyles, K. A. Kaihara, F. Vaida, R. T. Schooley, *J. Virol.* **2007**, *81*, 3005.
[17] T. Kato, T. Date, M. Miyamoto, A. Forsake, K. Tokushige, M. Mizokami, T. Wakita, *Gastroenterology* **2003**, *125*, 1808.
[18] S. Hopkins, B. Scorneaux, Z. Huang, M. G. Murray, S. Wring, C. Smitley, R. Harris, F. Erdmann, G. Fisher, Y. Ribeill, *Antimicrob. Agents Chemother.* **2010**, *54*, 660.
[19] C. J. Halfman, *Methods Enzymol.* **1981**, *74*, 481.

SUPPORTING INFORMATION

Additional supporting information may be found online in the Supporting Information section at the end of the article.

How to cite this article: Ramsis TM, Abdel Karim SE, Vassilaki N, et al. Expanding the chemical space of anti-HCV NS5A inhibitors by stereochemical exchange and peptidomimetic approaches. *Arch Pharm Chem Life Sci*. 2018;1–10. https://doi.org/10.1002/ardp.201800017